Journal of Low Temperature Physics, Vol. 25, Nos. 3/4, 1976

Spin Properties of Conduction Electrons in Sodium

J. M. Perz* and D. Shoenberg

Cavendish Laboratory, Cambridge, England

(Received March 1, 1976)

It was found that very carefully prepared Na crystals gave quite large-amplitude de Haas–van Alphen oscillations, as if little or none of the metal had undergone the martensitic transformation in cooling to liquid helium temperatures. Detailed study of the absolute amplitude and the harmonic content of the oscillations gave the ratio of the spin susceptibility to that of a free electron gas as $\chi/\chi_0 = 1.632 \pm 0.007$, *the spin-splitting factor as* $g = 2.636 \pm 0.024$, *and the parameter* B_0 *in Fermi liquid theory as* $B_0 = -0.241 \pm 0.007$. *These determinations are appreciably more accurate than earlier ones, and are consistent with them and agree well with recent theoretical estimates. In the analysis of the observed oscillations it was necessary to take account of strong magnetic interaction effects, particularly at 0.6 K, and the results provide some evidence for a modified form of the theory of magnetic interaction in the presence of significant phase smearing.*

1. INTRODUCTION

Recent studies by Randles[1] and Knecht[2] have demonstrated that measurements of oscillation amplitudes in the de Haas–van Alphen (dHvA) effect can be used to determine the spin susceptibility and the g-factor of the conduction electrons of a metal. These spin properties can differ appreciably from those of a free electron gas because of spin–orbit and many-body interactions. Both interactions are of comparable importance in the noble metals, but only the many-body interaction is appreciable in the alkali metals, so that the results are correspondingly simpler to interpret in terms of basic theory. So far only K, Rb, and Cs have been studied; because of the martensitic transformation, only feeble dHvA oscillations have been observed in Na[3–5] up to now and no dHvA effect has yet been observed in

*Permanent address: Department of Physics, University of Toronto, Toronto, Ontario, Canada.

crystalline Li.* We have recently succeeded in preparing single crystals of Na which gave considerably larger dHvA amplitudes than those reported earlier and this has made possible a determination of the spin characteristics of Na appreciably more accurate than those based on other methods.[7–9] The experiments have also provided interesting new evidence about the effect of magnetic interaction in the dHvA effect in the presence of phase smearing due to slight sample inhomogeneity. The improvements in sample preparation which made the experiments possible are described in Section 2.1; it is likely that these improvements inhibited the martensitic transformation (which normally occurs on cooling through 36 K) either partially or completely, thus providing good-quality single crystals of the high-temperature (bcc) phase at the low temperatures necessary to display the dHvA effect.

2. EXPERIMENTAL TECHNIQUES

2.1. Sample Preparation

The technique of sample preparation was in essence that described by Knecht,[2] in which a rod-shaped crystal was grown under oil in a glass capillary, which was sealed after removal of the oil. Experience showed, however, that unless great care was taken in handling before cooling to liquid helium temperatures, no dHvA oscillations were observed. This is in line with Barrett's observation[10] that the fraction of a Na sample that undergoes the martensitic transformation to the hcp phase at about 36 K depends strongly on the initial degree of strain in the sample and that if the sample is carefully handled and no deliberate strain introduced, the fraction transforming can be reduced to as little as 5%. Presumably, then, samples that have been accidentally damaged by awkward handling transform sufficiently to reduce considerably the amplitude of the dHvA effect.†

Another factor which appeared to be important in obtaining good dHvA oscillations was the procedure of cooling the sample through the martensitic transformation point. Experience suggested that rapid cooling was essential and that it was important to avoid temperature fluctuations which could carry the sample more than once through the transformation point.

*Feeble oscilations,[6] corresponding to an average over crystal orientations, have been seen in colloidal Li; although in principle the amplitude of these oscillations could be used to give information about spin properties, this has not yet been done.

†Reduction of amplitude in a sample that has undergone partial or total transformation would be expected both because the hcp phase would not all have the same orientation, and because any remaining bcc phase might be considerably and inhomogeneously strained by the material that had transformed, thus causing reduction of amplitude through phase smearing.

To grow a crystal, a small length (typically 3 mm) of molten Na was introduced into a slightly longer glass capillary of uniform bore (typically 1 mm diameter) by means of a hypodermic syringe under oil. The crystal was then grown by laying the capillary horizontally in the oil bath and cooling the bath at about $\frac{1}{2}$ C per minute with a temperature gradient of order 0.01 C per mm along the capillary. After cooling to room temperature the capillary was very gently removed from the bath and excess oil removed by suction with a hypodermic syringe, followed by gentle washing with heptane (checking that the sample could move freely in the capillary during this washing). The heptane was then sucked out and the last traces removed by evaporation under rough vacuum. Finally, short lengths of terylene fishing line were inserted at the two ends to hold the sample in place and the ends sealed with epoxy resin to prevent access of air. Initially, all this was done in a glove box in dry helium, but it proved difficult to avoid clumsy handling and eventually it was found better to do the necessary handling operations in the open and put up with the consequent slight corrosion at the ends of the sample.

The sealed-off samples were examined both visually under a microscope and by transmission Laue x-ray photography. There proved to be a fair degree of correlation between nonappearance of dHvA oscillations and observation of slight cracks and wrinkles under the microscope on the one hand and of Laue spots broken up into clusters (spread over a few degrees) on the other. Thus eventually only samples showing no visible damage and giving sharp Laue spots were chosen for cooling to liquid helium temperatures and these did in fact nearly always give good dHvA oscillations.

The sample volume was determined by direct measurement of the dimensions (the diameter being taken as that of the capillary bore before filling, less a small correction for shrinkage on solidification) with due allowance for the rounded ends; the room-temperature volume was reduced by a factor 0.955 to allow for thermal contraction. For some of the samples the volume was also determined by the eddy current method described by Knecht,[2] and was usually found to be consistent with the other estimate to within 10% or so, which is of the same order as the joint uncertainty of both determinations. This shows that there are no appreciable cavities in the samples. The eddy current determination was made on only one of the two samples (sample 16) which gave the most reliable results and the volume was found to be 8% lower than that estimated from the dimensions (this lower volume was used in the reduction of the data).

2.2. Measurement and Analysis of the dHvA Amplitudes

The field modulation technique (see, for instance, Ref. 11) was used with detection at the modulation frequency, so that the deflection of the

output chart recorder is proportional to dM/dH and the oscillatory variation of dM/dH with H is displayed as H is slowly swept. The oscillations of dM/dH were also recorded digitally on paper tape, from which their Fourier components could be computed. The constant of proportionality between the output of the recording system and dM/dH was determined as described by Knecht.[2] The only other feature of the technique that needs mention is that the very high conductivity of Na necessitated the use of very low modulation frequencies (typically between 5 and 10 Hz) to avoid the eddy current complications discussed by Knecht.

The connection between the dHvA amplitudes and the spin properties comes through the Lifshitz–Kosevich (LK) formula, which specifies the amplitudes a_r of the Fourier components of the oscillations in the form [see (A3) and (A4) of the appendix]

$$a_r = f(H, T, r)G_r \tag{1}$$

where

$$G_r = \cos[(r\pi/2)gm/m_0] = \cos[r\pi(g_0^2/2g_s)(\chi/\chi_0)] \tag{2}$$

m/m_0 is the ratio of the cyclotron mass to the free electron mass, χ/χ_0 is the ratio of the spin susceptibility of the conduction electrons to that of a free electron gas, g_0 is the free electron value (2.0023), and g_s the CESR value (2.0015); the difference of the factor $g_0^2/2g_s$ from unity is small but just significant. Note that the value of G_1 automatically specifies all the other G_r. Thus in principle the spin properties (i.e., the G_r and hence χ/χ_0 or g) can be determined if the a_r are known. However, we have so far ignored magnetic interaction (MI), which comes about because the effective field in the metal is B rather than H. Because of MI the a_r of (1) are related in a complicated way to the harmonic amplitudes actually observed. This problem can be dealt with fairly simply if the MI is weak enough, as it was in Knecht's experiments on the other alkali metals, but more elaborate procedures are needed to deal with the appreciably stronger MI that is found in Na, particularly at very low temperatures. These procedures are outlined in Section 3 and more fully described in the appendix; some interesting novel aspects of the theory appear when MI and phase smearing are both important.

3. EXPERIMENTAL RESULTS

The dHvA oscillations were successfully observed with six samples (one of which showed undiminished amplitudes in a second run, even though it had been warmed to room temperature in between) and about as many gave no oscillations at all. Nearly always the negative experiments could be

correlated with evidence of slight damage to the sample or with too slow cooling to low temperature. The early experiments were somewhat exploratory in character and suffered from various unsatisfactory features which were gradually eliminated as experience was gained. Thus in the first few experiments there was some doubt about the field homogeneity and the modulation frequency was not quite low enough to ensure freedom from eddy current effects. Again, some samples showed rather high Dingle temperatures with not very straight Dingle plots and in some there was clear evidence that not all the sample volume was effective (which implies uncertainty in the demagnetizing coefficient). However, in spite of these doubtful aspects, the preliminary experiments made it likely that the amplitude-determining factor G_1 [see (2)] lay between 0.35 and 0.45 and thus provided a helpful guide in the interpretation of the two best experiments, one at 1.2 K and the other at 0.6 K. Only these two experiments will be discussed further.

3.1. The Experiment at 1.2 K (run 11, sample 12)*

A few oscillations at the highest field (84.9 kG) are reproduced in Fig. 1 and show the sharpened peaks and broadened bottoms characteristic of fairly strong MI. From Fourier analysis of the digitized recordings of a few oscillations at each of a number of fields down to about 35 kG, the

*This sample contained a small percentage of K (probably less than 0.05%), introduced in the hope that it might help to inhibit the martensitic transformation. From details of the eddy current behavior at liquid helium temperatures it could be inferred that the resistivity of the sample was still very low and not high enough to cause any appreciable contribution to the Dingle temperature.

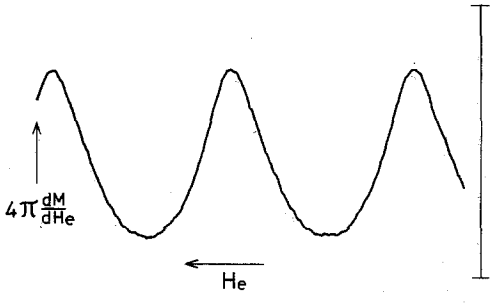

Fig. 1. Recorder trace at 84.9 kG and 1.2 K. The length of the vertical line on the right indicates a change of $4\pi\, dM/dH_e = 1$, assuming that all the sample volume is effective. The period of one oscillation is 25.5 G.

amplitudes R_r and phases* ϕ_r for each field were determined in the relation

$$4\pi\, dM/dH_e = \sum_r R_r \sin(rkh + \phi_r) \tag{3}$$

where h is the difference of the field from some arbitrary reference field H_0 in the range of observation and $k = 2\pi F/H_0^2$. The R_r and ϕ_r are adjusted to allow for the finite modulating field and for the time constant of the recording system (these adjustments become appreciable at low fields and for high r) and R_r is defined to be positive. Note that in (3) we distinguish between H_e, the "external" field, and the H field in the metal; the relation between them is

$$H = H_e - 4\pi nM \tag{4}$$

so that

$$B = H_e + 4\pi(1-n)M \tag{5}$$

where $4\pi n$ is the demagnetizing coefficient of the sample (for this sample $n = 0.10$).

As explained more fully in the appendix, the LK formulation in effect expresses M as a function of B, so that the relation between M and H_e becomes a complicated implicit one. When MI is not too strong (in the sense that the amplitude of $4\pi\, dM/dB$ as given by LK is appreciably less than one), this implicit relation can be solved to give M as an explicit function of H_e by an iterative procedure due to Phillips and Gold[12] (PG). This solution can be summarized in the form

$$4\pi\, dM/dH_e = \sum_r c_r |a_1^r| \sin(rkh + \psi_r) \tag{6}$$

where a_1 is the fundamental amplitude in the LK formula and c_r and ψ_r are rather complicated functions of the a_r (and of the Dingle temperature x and the demagnetizing coefficient n), as specified in the appendix; note that c_r is defined to be positive.

If a_1 is small enough (i.e., for weak MI) and all a_r for $r > 2$ can be neglected, as was usually the case in Knecht's experiments, the expressions for c_1, c_2, ψ_1, and ψ_2 become relatively simple and comparison of (6) and (3) can be used to yield estimates of a_1 and a_2 in several different ways. However, for the stronger MI and the stronger a_2 and a_3 of Na, Knecht's approximation is not quite accurate enough, and because of the complicated way in which the c_r involves the a_r we adopt a trial and error procedure. In

*The phases ϕ_r depend of course on the origin of h, but the differences $\phi_r - r\phi_1$ are independent of this origin.

this procedure a trial value of G_1 (and thus of all the other G_r) is *assumed*, which, by way of the LK formula, determines the a_r and hence the c_r and ψ_r. As is explained in the appendix, there are two extreme variants of the MI theory. In the conventional or "old" treatment, MI is applied to the a_r, in which the Dingle factor γ^r has been included, where*

$$\gamma = \exp(-2\pi^2 kx/\beta H) \tag{7}$$

β is $e\hbar/mc$ and x is the Dingle temperature, so that a value of x is required to determine the a_r. In the "new" treatment, however, MI is applied to the a_{r0}, in which the Dingle factor is omitted, and the phase smearing that produces the Dingle factor is applied only *after* the MI; the result of this procedure still has the form (6) but the c_r are now independent of x and are completely determined once G_1 is assumed.

Some graphs showing the field dependence of several of the c_r and ψ_r on various assumptions are shown in Figs. 2 and 3. Once the c_r, which are in a sense "correction factors," are known, comparison of (3) and (6) gives

$$c_r|a_1^r| = R_r \tag{8}$$

and we see that a_1 for any given field can be determined in a variety of ways.

In the "absolute amplitude" (AA) method, in which we require absolute calibration of the recording equipment and also the sample volume, we use R_1 and find a_1 as

$$|a_1| = R_1/c_1 \tag{9}$$

A plot of $\ln(a_1 H^{5/2})$ against $1/H$ from the a_1's obtained in this way using the trial value $G_1 = 0.4$ is shown in Fig. 4 and it can be seen that this Dingle plot is indeed a good straight line, confirming the exponential law assumed in the theory. The slope of the plot gives $T+x$ and we find

$$x = 0.23 \text{ K} \tag{10}$$

and the intercept gives the value of

$$\ln(4.11 \times 10^{-4} F^2 T G_1) \tag{11}$$

where F is the dHvA frequency and the Fermi surface has been assumed spherical. From (11) we find $G_1 = 0.36$. This estimate is insensitive to the trial value of G_1 used in deriving c_1, but it is inversely proportional to the assumed volume, which unfortunately is not known to better than 5% or so. In any case the AA method as applied to Na probably sets only a lower limit to G_1, because a fraction of the sample may have undergone the martensitic

*For Na, $m/m_0 = 1.24$ and (7) becomes $\gamma = \exp(-1.822 \times 10^5 x/H)$.

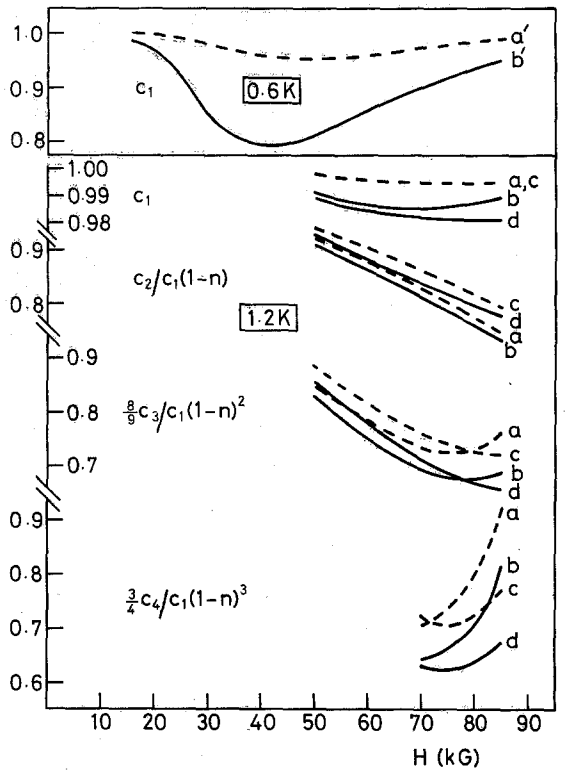

Fig. 2. Field dependence of the c coefficients. The quantities plotted are defined to approach unity in the limit of low fields. At 1.2 K all the quantities are calculated for $1-n = 0.9$; curves a and b are for $G_1 = 0.38$, while c and d are for $G_1 = 0.42$. The broken lines (a, c) refer to the old treatment of MI, the solid lines (b, d) to the new. At 0.6 K only c_1 is shown for $1-n = 0.92$ and $G_1 = 0.40$; as above, the broken line (a') refers to the old and the solid line (b') to the new treatment; in the new treatment c_1 decreases by roughly 2% for 5% increase in G_1.

transformation and so become ineffective. In some of the earlier experiments the AA estimates of G_1 were as low as 60% of those obtained by the MI method to be described below, which are independent of the sample volume and of the calibration of the recording equipment.

In the MI method, we use (8) to give

$$|a_1| = [(R_r/R_1)(c_1/c_r)]^{1/r-1} \tag{12}$$

so that for any trial value of G_1 (which determines c_1/c_r) a value of a_1 can be deduced from the experimentally observed ratio R_r/R_1, which does not

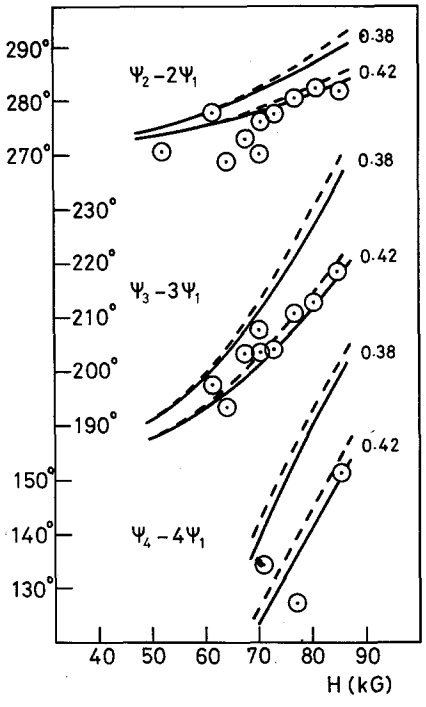

Fig. 3. Field dependence of phase of the harmonics at 1.2 K. The broken lines are calculated by the old treatment and the solid lines by the new treatment of MI for the trial values of G_1 indicated. At sufficiently low fields the phases $\psi_2-2\psi_1$, $\psi_3-3\psi_1$, and $\psi_4-4\psi_1$ should approach 270, 180, and 90°, respectively. The circles are the experimental points, as corrected for the time constant of the recording system. Below 70 kG a shorter time constant was used, with a consequent increase in noise; this is probably the cause of the greater scatter of the points below 70 kG.

involve the sample volume or the calibration constants. For self-consistency any such estimate of a_1 should agree with the theoretical value of a_1 based on the assumed value of G_1 and the value of Dingle temperature x already determined, i.e.,

$$|a_1| = 4.11\times10^{-4}F^2TG_1H^{-5/2}\exp[-2\pi^2k(T+x)/\beta H] \qquad (13)$$

Effectively, (13) is equivalent to the absolute value of a_1 determined from the fundamental amplitude as described above but with the sample volume adjusted to give the assumed value of G_1. The degree of consistency is best assessed by comparison of direct, rather than logarithmic, plots of the field dependence of a_1 as determined by (12) and by (13) and this is shown in Fig. 5 for the alternative assumptions $G_1 = 0.38$ and 0.42. Bearing in mind the weakness of the harmonics,* the agreement between the estimates of a_1

*At 85 kG, $R_2/R_1 = 0.24$, $R_3/R_1 = 0.085$, and $R_4/R_1 = 0.0375$, while at 52 kG, $R_2/R_1 = 0.13$ and $R_3/R_1 = 0.036$; these figures have been corrected for finite modulation and time constant effects, so that the harmonics actually observed are even weaker.

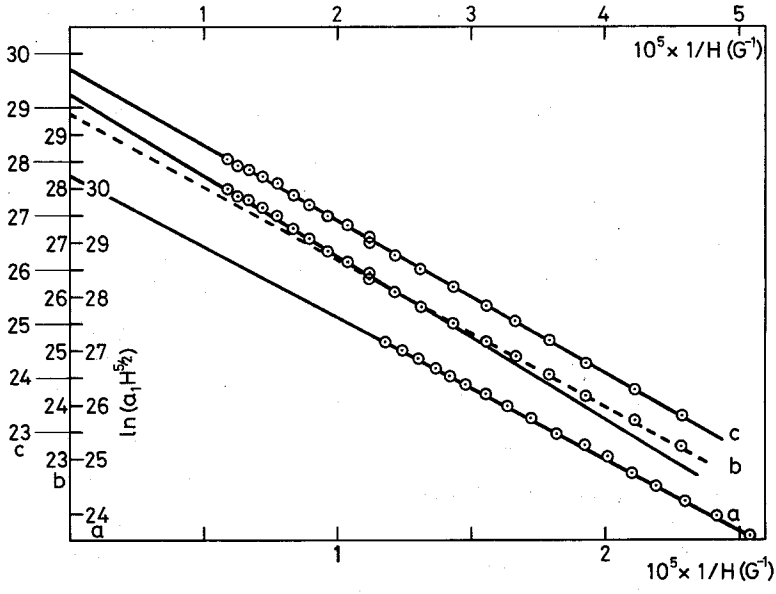

Fig. 4. Dingle plots of $\ln(a_1 H^{5/2})$ against $1/H$ calculated assuming $G_1 = 0.4$ (a) 1.2 K, with c_1 calculated by the new treatment; (b) 0.6 K, with c_1 calculated by old treatment; the solid straight line is drawn through the upper field points, the broken one through the lower field points; (c) 0.6 K, with c_1 calculated by new treatment; note the improved linearity. The lower scale of $1/H$ refers to curve a and the upper to b and c. Appropriate correction has been made to allow for the difference of exp and 2 sinh (the correction is negligible at 1.2 K).

based on the second, third, and even the fourth harmonics is very satisfactory. Comparison with the "absolute" curves, i.e., based on (13), particularly at high fields where the MI method is most accurate, suggests that G_1 is between 0.38 and 0.42, but closer to 0.42 than to 0.38.

Further evidence comes from the phases of the harmonic components relative to the fundamental. It is easily seen from (3) and (6) that the appropriate comparison is between the observed values of $\phi_r - r\phi_1$ and the calculated values of $\psi_r - r\psi_1$. The graphs of Fig. 3 show that there is very satisfactory agreement between the observed and predicted field dependence of the phases and once again that G_1 is probably closer to 0.42 than 0.38 if the new treatment of MI is used. It can be seen, too, that had the conventional treatment of MI been used (i.e., MI after, rather than before, phase smearing) a slightly higher value of G_1 (perhaps 0.01 higher) would have been needed to give agreement between observed and predicted phases. It should be noticed that because of the complexity of the relation (6) when the PG iterative procedure is taken to sufficiently high order of

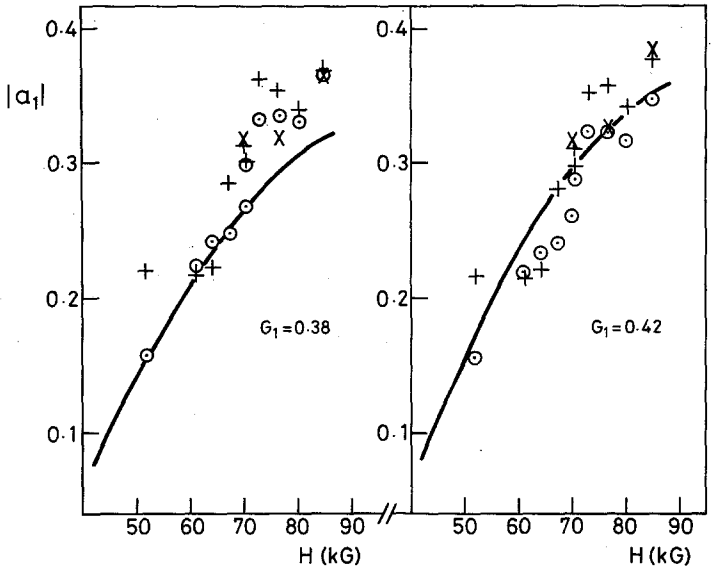

Fig. 5. Field dependence of $|a_1|$ at $T = 1.2$ K for the trial values $G_1 = 0.38$ and 0.42. The solid curves are calculated from (13) for $x = 0.23$ K. The points are derived from the experimentally observed ratios of harmonic amplitudes ("MI method") as follows: ⊙ from R_2/R_1, + from R_3/R_1, × from R_4/R_1. To avoid confusion, only the points based on the new treatment are shown; on the old treatment the ⊙ and × points would move down by about 2 and 4%, respectively and most of the + would move up by about 2%; these changes are not very significant on the scale of the diagram.

approximation, it is no longer a straightforward matter to apply Knecht's "harmonic ratio" (HR) method, in which a_2/a_1 is derived from the observed R_1/R_2, ϕ_1, and ϕ_2. However, the comparison of phases that has just been discussed in a sense replaces the HR method in providing an independent method of estimating G_1.

3.2. The Experiment at 0.6 K (run 12, sample 16)

As can be seen from Figs. 6 and 7, not only is MI very strong over a wide field range at this lower temperature, but the line shape at the higher field is evidently strongly influenced by the LK harmonics. It is still possible to use the PG iterative procedure to estimate c_1 in (6), and hence a_1 from R_1, so that the AA method can be used to find G_1 from the intercept of the Dingle plot (see Fig. 4b, c). Using the trial value* $G_1 = 0.4$, the AA method gives $G_1 = 0.42$, which is very reasonably consistent with the estimate based on

*An increase of 5% in the trial value of G_1 would increase the result of the AA method by roughly 2 or 3%, but would not significantly change the Dingle temperature.

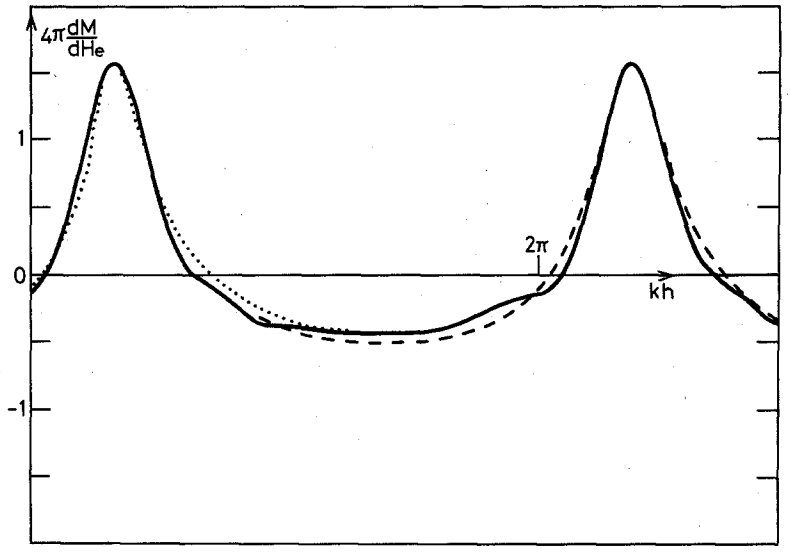

Fig. 6. Oscillation of $4\pi\, dM/dH_e$ with field at 0.6 K and 51.9 kG; here h is the difference of H_e from an arbitrary origin H_0 and $k = 2\pi F/H_0^2$. Solid curve: experimental, reconstituted from Fourier analysis of digitized record after correcting harmonic amplitudes for finite modulation current and for time constant (the latter correction almost negligible). Dotted curve: Theory, old treatment, $G_1 = 0.38$, $x = 0.22$ K or $G_1 = 0.42$, $x = 0.25$ K. Dashed curve: Theory, new treatment, $G_1 = 0.38$, $x = 0.14$ K or $G_1 = 0.42$, $x = 0.16$ K. The difference between the alternatives is too slight to show clearly on the scale of the diagram.

the higher temperature experiment; this consistency shows that no appreciable fraction of the sample has become ineffective through the martensitic transformation. It is also evident from Fig. 4 that the Dingle plot based on the new version of MI theory (i.e., MI applied before rather than after phase smearing) is much more linear than that based on the old version; this suggests that the new version is the more correct, though probably new and old should be regarded in some sense as extreme approximations. The value of the Dingle temperature is found to be $x = 0.17$ K.

The use of the PG iterative procedure to interpret the higher harmonic amplitudes and phases proves rather inconclusive because of insufficiently rapid convergence. Indeed, the validity of the PG procedure for values of a_1 comparable to unity becomes uncertain because it ignores the possibility of domain formation over part of each cycle when the amplitude is large enough (as it is, using the new version of MI theory). In fact trial values of G_1 around 0.4 did give reasonable estimates of a_1 by the MI method as applied to the observed ratio R_2/R_1, but the estimates still changed by something

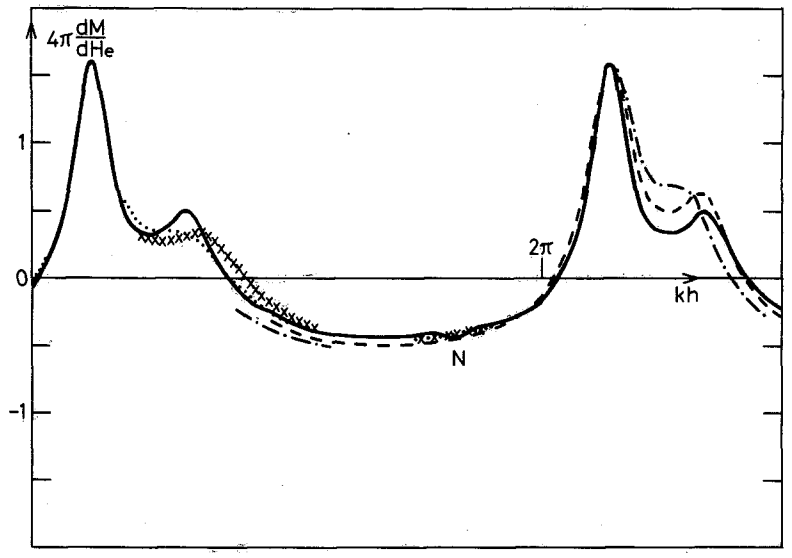

Fig. 7. Oscillation of $4\pi\, dM/dH_e$ with field at 0.6 K and 84.8 kG; k and h as in Fig. 6. (—) Experimental, reconstituted as in Fig. 6. (×××) Theory, old treatment, $G_1 = 0.38$, $x = 0.25$ K. (· · ·) Theory, old treatment, $G_1 = 0.42$, $x = 0.28$ K. (– – –) Theory, new treatment, $G_1 = 0.38$, $x = 0.15$ K. (– · – · –) Theory, new treatment, $G_1 = 0.42$, $x = 0.16$ K.

like 10% when the PG procedure was carried to eighth rather than sixth order, and moreover the phase comparison was out by something like 10° at the highest field.

It was therefore decided to try an alternative approach, that of trial and error synthesis. As before, a trial value of G_1 was assumed and the LK formula applied to compute the oscillation of M as a function of B (without any Dingle factor on the new treatment, but including a Dingle factor γ^r for the rth harmonic on the old treatment). From the M–B relation, the M–H_e relation can be immediately computed, since H_e is given by (5) and also the dM/dH_e vs. H_e relation, since it follows from (5) that

$$dM/dH_e = (dM/dB)/[1-4\pi(1-n)\, dM/dB] \tag{14}$$

On the old treatment the dM/dH_e vs. H_e relation obtained in this way is the one to be compared directly with experiment. On the new treatment, however, the procedure is more complicated. First, the amplitudes can be so large (because no Dingle factor has been included) that the M–H_e curve becomes S-shaped (as in Fig. 8), and over the range A to B, the sample should break up into domains with a linear dependence of M on H_e; the value of $4\pi\, dM/dH_e$ over this range should be $1/n$, which for this sample is

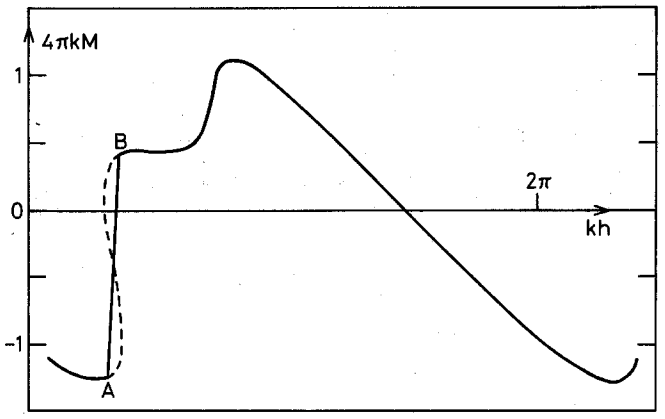

Fig. 8. Theoretical magnetization curve for 0.6 K and 84.8 kG after MI, but assuming a perfect sample (zero Dingle temperature); k and h as in Fig. 6. The broken part of the curve is not realized; instead M follows the straight line AB, which cuts off equal areas and has slope $1/n$, which is 12.5 for this sample.

12.5. Second, the harmonics of the M–H_e oscillation (modified to allow for the domain region, as in Fig. 8) now need to be damped by the factors γ^r; the harmonics are found by Fourier analysis* and after multiplication by γ^r they are resynthesized to give the final oscillation line shapes of M and dM/dH_e.

The results of these procedures are compared with the experimental curves in Figs. 6 and 7 for the trial values $G_1 = 0.38$ and 0.42 and for various values of the Dingle temperature x (and hence of γ) chosen to give the best fit to the height of the maximum of the oscillation; it can be seen that the best synthetic curves do reproduce the observed curves fairly well. In comparing the various curves with the observed ones, it should be remembered that the Dingle plot of Fig. 4 indicates a Dingle temperature of $x = 0.17$ K (using the new treatment, since the old did not give a linear plot) and it can be seen that the values of x that give the best fits in Figs. 6 and 7 are closer to 0.17 using the new treatment than those using the old treatment. However, the old treatment gives a rather better fit than the new over the long, flat, negative region at both high and low fields. At the lower field there is little to choose between the two trial values of G_1, though on the new treatment 0.42 gives the values of x closest to 0.17. At the higher field none of the calculated

*Because the computation of the M–B curve was made at equal intervals of B, the intervals of H_e are unequal and the Fourier analysis was done by the laborious (and not too precise) process of digitizing the dM/dH_e vs. H_e computer plot at equal intervals of H_e and then using the standard program for Fourier analysis.

curves reproduces the subsidiary peak quite faithfully, but it is best reproduced for $G_1 = 0.38$ on the new treatment. It should also be pointed out that values of G_1 outside the range from 0.38 to 0.42 give worse fits than those illustrated, particularly as regards the position of the subsidiary peak.

The lack of perfect fit between calculated and observed curves may be partly due to relatively trivial experimental causes (e.g., noise, such as at N in Fig. 7, errors of up to a few percent in absolute scale, and errors in allowances made for time constant and finite modulation current). Moreover, the data used in computing the synthetic curves are all subject to appreciable errors (say 1% in m and F, 3% in T, and 2% in $1-n$). However, probably the main cause for the discrepancies is inadequate reliability of the theory used in the calculations.

First of all both the new and old versions of MI theory are in a sense limiting approximations, and though the new treatment is probably the better approximation, it may well be appreciably imperfect. An obvious suggestion is to try an intermediate version in which one damping factor γ_1 is introduced before MI and a second, γ_2, after MI, with the product $\gamma_1\gamma_2$ corresponding to the overall Dingle factor. After some trial and error a very good fit at the high field was found for the particular combination $\gamma_1 = 0.825$ and $\gamma_2 = 0.78$ (this corresponds to $x = 0.20$ K) for $G_1 = 0.38$ (the difference between the calculated and observed curves would not show on the scale of Fig. 7). No doubt equally good fits could be obtained for somewhat different combinations of $\gamma_1\gamma_2$ and G_1 (though it did not seem possible to get the subsidiary peak right with $G_1 = 0.42$), but there is probably little point in getting a perfect fit in this way, because of the arbitrariness of introducing an extra parameter and also because the theory may be unreliable in a second respect.

The second point is that phase smearing by multiplication with γ^r may not be quite right and indeed is justified only if the phase distribution is strictly Lorentzian, for which there does not appear to be any sound basis, except the linearity of the Dingle plot, which may not be quite exact. The difficulty of getting a good fit around the subsidiary peak could probably be remedied if there was freedom to introduce less severe damping for the higher harmonics, but once again there is little point in improving the fit by ad hoc assumptions without any theoretical basis.

4. DISCUSSION

4.1. Summary of Experimental Conclusions

Analysis of the observed harmonic amplitudes and phases at 1.2 K suggests that G_1 is closer to 0.42 than to 0.38 and lies between them. The

experiment at 0.6 K is consistent with this conclusion, though it does not help to narrow the range of uncertainty in G_1, partly because the uncertainties of how to deal with MI and phase smearing are more sensitively involved in the interpretation than they are at 1.2 K. A conservative conclusion consistent with both experiments and with the uncertainties of the theory is that*

$$G_1 = 0.41 \pm 0.02 \tag{15}$$

The experiments also demonstrate that the LK theory, corrected for MI, with phase smearing as γ^r after MI, gives a very good account of the detailed line shape, amplitude, and phase of the oscillations over a wide range of fields at both 0.6 and 1.2 K. In principle G_1 might of course vary with crystal orientation, but no large anisotropy is to be expected on theoretical grounds and the present experiments are too insensitive to demonstrate any anistropy smaller than a few percent.

4.2. Interpretation of G_1

From the definition of G_1 [see (2)], we find that possible values of χ/χ_0 consistent with $G_1 = 0.41$ are

$$\chi/\chi_0 = 0.365,\ 0.633,\ 1.364,\ \underline{1.632},\ 2.362, \text{ etc.} \tag{16}$$

i.e., $0.9984(l \pm 0.366)$, where l is an integer (in principle l could also be negative).

In the absence of any information on the absolute phase of the oscillations (which could exclude either odd or even values of l), the only guide to a choice among the various possibilities is comparison with other determinations. Other experimental determinations are of Dunifer *et al.*[7] (DPS) by the spin-wave method, giving $\chi/\chi_0 = 1.58 \pm 0.09$; of Schumacher and Vehse[8] based on CESR, giving 1.72 ± 0.08; and of Dupree and Seymour[9] based on direct susceptibility measurements (with theoretical allowance for diamagnetic and ionic contributions), giving 1.62 (no error is stated, but the uncertainties in the allowances are probably considerable). All these clearly point to the underlined value in (16) and putting in the ± of (15), our result becomes

$$\chi/\chi_0 = 1.632 \pm 0.007 \tag{17}$$

which is consistent with all the earlier experimental determinations. The good precision of our determination is partly due to the fact that the

*The quoted ± is a rather subjective estimate of the uncertainty but it is intended in the sense of a standard deviation. Thus for the two best experiments none of the various ways of estimating G_1 indicates a value outside the range 0.37–0.45.

experimental contribution to χ/χ_0 is only the 0.366 part, i.e., less than one-fourth of the total, while the contribution 0.9984×2 is of course almost exact, and partly because G_1 has a value for which the relative error in $\cos^{-1} G_1$ is only about 0.4 that of G_1; thus the $\pm 5\%$ uncertainty in G_1 is reduced to less than $\pm\frac{1}{2}\%$ in χ/χ_0. Our estimate of χ/χ_0 agrees remarkably well with recent theoretical estimates, particularly with one by Vosko *et al.*,[13] who find 1.62 using a spherical cell approximation (references to earlier calculations are given in their paper and in that of Knecht[2]). A more recent calculation using the bcc cell gives 1.64.[17]

Our result can also be expressed in terms of g [see (2)] and if we put $m/m_0 = 1.24 \pm 0.01$, we find

$$g = 2.636 \pm 0.024 \tag{18}$$

According to Fermi liquid theory,

$$g = g_s/(1+B_0) \tag{19}$$

where B_0 is the zeroth-order parameter of the theory and g_s is the CESR value, which is 2.0015 for Na. Thus we find

$$B_0 = -0.241 \pm 0.007 \tag{20}$$

Since it is B_0 which is directly determined by the spin-wave method, it is useful to compare our value of B_0 with that of DPS, who find -0.215 ± 0.03. Although the two values are consistent within the experimental errors, the possibility should not be excluded that the difference between them is significant and arises from oversimplifications in the applications of Fermi liquid theory to two quite different phenomena.

APPENDIX

The problem of magnetic interaction is intimately linked with the question of the origin of the Dingle factor γ [see (7)]. If this factor is due to broadening of the Landau levels, such as caused by impurity scattering, γ appears directly in the LK relation between M and B [see (A1) and (A3) below] and the conventional treatment of translating the implicit relation between M and H_e into an explicit one is correct. Often, however, and probably in the present Na samples, the origin of γ is quite different; it is due to some kind of phase variation in the sample—for instance, caused by variations of strain—rather than to a uniform broadening of the Landau levels. It is then more appropriate to think of the sample as a mosaic of regions, within each of which the phase is nearly constant, but with a

variation of phase from one region to another. This presents a very complicated interaction problem since the local M of each region affects the field in its neighbors and the usual assumption of a uniform M is no longer valid.

It turns out, however, that a very simple approximate treatment[14] agrees remarkably well with some recent experiments[15] on strong interaction in gold and some theoretical justification can indeed be found for this approximation under certain simplifying assumptions. The approximation is to suppose that each region can be treated as if it were perfect (i.e., $\gamma = 1$) and of the same shape as the whole sample. The interaction problem is then solved for this region as if it were isolated to give the local M as a function of H_e. The phase variation between one region and another is then put in by applying the factor γ^r to the rth harmonic of the M–H_e relation for the perfect region. We shall not discuss the merits of this new approach further here, but now present the MI theory in a form such that both the conventional (γ introduced before MI) and the new (γ after MI) treatment are included in the same treatment.

In the conventional treatment, the LK formula* for a convex Fermi surface can be conveniently expressed as

$$4\pi M = \sum_{r=1}^{\infty} \frac{a_r}{kr} \sin\left(\frac{2\pi rF}{B} - \frac{\pi}{4}\right) \tag{A1}$$

where

$$k = 2\pi F/H^2 \tag{A2}$$

$$a_r = a_{r0}\gamma^r \tag{A3}$$

$$a_{r0} = \frac{-2.054\times 10^{-4} F^2 T r^{1/2} G_r}{H^{5/2} \sinh\left[1.469\times 10^5 (m/m_0) rT/H\right]} \tag{A4}$$

$$\gamma = \exp\left[-1.469\times 10^5 (m/m_0) x/H\right] \tag{A5}$$

and G_r is as defined in (2), i.e.,

$$G_r = \cos\left[(r\pi/2) gm/m_0\right] \tag{A6}$$

The problem of MI is that (A1) is an *implicit* equation for M since

$$B = H_e + 4\pi(1-n)M \tag{A7}$$

and this has to be solved to give an explicit relation between M and H_e.

*The difference between B and H_e (and between H_e and H) is significant only in the argument of the sine (because of its very high phase), and can be ignored in all the modulating factors; it is therefore entirely justified to use H rather than B in (A2), (A4), and (A5). The notation here is slightly different from that of PG; thus their A_r and κ are related to our a_r and k by $a_r = r\kappa A_r$ and $\kappa = 4\pi k$. The numerical coefficient in the numerator of (A4) assumes a spherical Fermi surface.

If MI is not too strong, the solution can conveniently be obtained by an iterative method due to Phillips and Gold.[12] Their result, generalized to allow for the sample shape, and given in terms of dM/dH_e rather than M, can be expressed to the lth approximation as

$$4\pi\frac{dM}{dH_e}=-\sum_{r=1}^{l}\left[P_r\cos\left(rkh+\frac{\pi}{4}\right)+Q_r\sin\left(rkh+\frac{\pi}{4}\right)\right] \tag{A8}$$

where the P_r and Q_r are the rather complicated functions of the a_r set out below, and h is the field difference from an appropriate reference field in the range of interest. Equation (A8) is of course equivalent to (6) if we put

$$c_r|a_1^r|=|(P_r^2+Q_r^2)^{1/2}| \tag{A9}$$

and*

$$\psi_r=(\pi/4)+\tan^{-1}(P_r/Q_r) \tag{A10}$$

The P_r and Q_r are related to the p_r and q_r of PG by

$$P_r=\kappa r p_r' \qquad \text{and} \qquad Q_r=\kappa r q_r' \tag{A11}$$

where the p_r' and q_r' are obtained from the p_r and q_r of PG by changing their κ to $\kappa(1-n)$ wherever κ appears in their Table II.

For our purposes it was necessary to carry out the iteration process to higher order than given by PG (their Table II stops at the fourth order) and this proved to be relatively simple using the CAMAL algebra system[16] developed in the Cambridge University Computer Laboratory.

It is convenient to express the resulting expressions for P_r and Q_r in terms of a_1^r and quantities α_r, which are defined by

$$\alpha_r=a_{r0}(1-n) \tag{A12}$$

We then have for $r=1$–4, but up to eighth-order approximation,

$$\begin{aligned}P_1=a_1\Bigg[1+\gamma^2\left(\frac{\alpha_2}{4\sqrt{2}}-\frac{\alpha_1^2}{8}\right)+\gamma^4\left(\frac{\alpha_1^4}{192}-\frac{\alpha_1^2\alpha_2}{48\sqrt{2}}-\frac{\alpha_2^2}{16}+\frac{\alpha_2\alpha_3}{12\sqrt{2}\,\alpha_1}\right)\\+\gamma^6\left(-\frac{\alpha_1\alpha_2\alpha_3}{96\sqrt{2}}-\frac{\alpha_1^2\alpha_4}{192\sqrt{2}}+\frac{\alpha_1^4\alpha_2}{1536\sqrt{2}}+\frac{\alpha_3\alpha_4}{24\sqrt{2}\alpha_1}\right.\\\left.-\frac{\alpha_2^3}{128\sqrt{2}}-\frac{\alpha_2^2\alpha_3}{96\alpha_1}-\frac{\alpha_3^2}{36}+\frac{\alpha_1^2\alpha_2^2}{128}-\frac{\alpha_1^6}{9216}\right)\Bigg]\end{aligned} \tag{A13}$$

*If the $\tan^{-1}$ is taken in the range $-\pi/2$ to $\pi/2$, then it is easily shown that an additional π should be added if Q_r is positive, but nothing if Q_r is negative.

$$Q_1 = a_1\Big[\frac{\gamma^2\alpha_2}{4\sqrt{2}} + \gamma^4\Big(-\frac{\alpha_1^2\alpha_2}{24\sqrt{2}} + \frac{\alpha_1\alpha_3}{24} + \frac{\alpha_2\alpha_3}{12\sqrt{2}\,\alpha_1}\Big) + \gamma^6\Big(-\frac{\alpha_1\alpha_2\alpha_3}{32\sqrt{2}} + \frac{\alpha_1^2\alpha_4}{192\sqrt{2}} + \frac{\alpha_1^4\alpha_2}{512\sqrt{2}} + \frac{\alpha_3\alpha_4}{24\sqrt{2}\alpha_1} - \frac{\alpha_2^3}{128\sqrt{2}} + \frac{\alpha_2\alpha_4}{32} - \frac{\alpha_1^2\alpha_2^2}{768} - \frac{\alpha_1^3\alpha_3}{384}\Big)\Big] \tag{A14}$$

$$P_2 = \frac{a_1^2(1-n)}{\sqrt{2}}\Big[\Big(-1 + \frac{\sqrt{2}\alpha_2}{\alpha_1^2}\Big) + \gamma^2\Big(\frac{2\alpha_3}{3\alpha_1} + \frac{\alpha_1^2}{3} - \sqrt{2}\,\alpha_2\Big) + \gamma^4\Big(\frac{\alpha_2^2}{8} - \frac{\alpha_1^4}{24} - \frac{\alpha_2^3}{4\sqrt{2}\,\alpha_1^2} - \frac{\sqrt{2}\,\alpha_2\alpha_3}{3\alpha_1} + \frac{\alpha_1^2\alpha_2}{2\sqrt{2}} + \frac{\alpha_2\alpha_4}{4\alpha_1^2} - \frac{\alpha_1\alpha_3}{3}\Big) + \gamma^6\Big(-\frac{\alpha_2^2\alpha_3}{12\alpha_1} + \frac{2\alpha_3\alpha_5}{15\alpha_1^2} + \frac{\alpha_3^2}{9} - \frac{\alpha_1\alpha_5}{15} - \frac{\alpha_1^2\alpha_2^2}{24} + \frac{\alpha_1^6}{360} - \frac{\alpha_2\alpha_4}{4} - \frac{\sqrt{2}\,\alpha_2\alpha_3^2}{9\alpha_1^2} + \frac{\alpha_1^3\alpha_3}{20} - \frac{\alpha_3\alpha_4}{3\sqrt{2}\,\alpha_1} + \frac{\alpha_2^3}{4\sqrt{2}} + \frac{\alpha_1\alpha_2\alpha_3}{3\sqrt{2}} - \frac{\alpha_1^4\alpha_2}{18\sqrt{2}}\Big)\Big] \tag{A15}$$

$$Q_2 = \frac{a_1^2(1-n)}{\sqrt{2}}\Big[1 + \gamma^2\Big(\frac{2\alpha_3}{3\alpha_1} - \frac{\alpha_1^2}{3}\Big) + \gamma^4\Big(-\frac{3\alpha_2^2}{8} + \frac{\alpha_1^4}{24} + \frac{\alpha_4}{2\sqrt{2}} + \frac{\alpha_1^2\alpha_2}{12\sqrt{2}} + \frac{\alpha_2\alpha_4}{4\alpha_1^2} - \frac{\alpha_1\alpha_3}{3}\Big) + \gamma^6\Big(-\frac{\alpha_2^2\alpha_3}{4\alpha_1} + \frac{2\alpha_3\alpha_5}{15\alpha_1^2} - \frac{\alpha_3^2}{9} + \frac{\alpha_1\alpha_5}{15} + \frac{\alpha_1^2\alpha_2^2}{8} - \frac{\alpha_1^6}{360} - \frac{\alpha_2\alpha_4}{4} + \frac{\alpha_1^3\alpha_3}{20} + \frac{\sqrt{2}\,\alpha_2\alpha_5}{5\alpha_1} - \frac{\alpha_1^2\alpha_4}{6\sqrt{2}} - \frac{\alpha_1^4\alpha_2}{60\sqrt{2}}\Big)\Big] \tag{A16}$$

$$P_3 = \frac{9}{8}a_1^3(1-n)^2\Big[\Big(\frac{8\alpha_3}{9\alpha_1^3} - \frac{\sqrt{2}\,\alpha_2}{\alpha_1^2}\Big) + \gamma^2\Big(\frac{9\alpha_2}{4\sqrt{2}} - \frac{3\alpha_2^2}{4\alpha_1^2} - \frac{2\alpha_3}{\alpha_1} + \frac{\alpha_4}{\sqrt{2}\,\alpha_1^2}\Big) + \gamma^4\Big(\frac{9\alpha_2^3}{16\sqrt{2}\,\alpha_1^2} + \frac{2\alpha_2\alpha_5}{5\sqrt{2}\,\alpha_1^3} - \frac{9\alpha_4}{8\sqrt{2}} - \frac{297\alpha_1^2\alpha_2}{320\sqrt{2}} - \frac{\alpha_2^2\alpha_3}{2\alpha_1^3} - \frac{3\alpha_2\alpha_4}{4\alpha_1^2} + \frac{27\alpha_2^2}{32} + \frac{9\alpha_1\alpha_3}{8}\Big)\Big] \tag{A17}$$

$$Q_3=\frac{9}{8}a_1^3(1-n)^2\Big[\Big(-1+\frac{\sqrt{2}\,\alpha_2}{\alpha_1^2}\Big)+\gamma^2\Big(-\frac{9\alpha_2}{4\sqrt{2}}+\frac{9\alpha_1^2}{16}+\frac{\alpha_4}{\sqrt{2}\,\alpha_1^2}\Big)$$
$$+\gamma^4\Big(-\frac{9\alpha_2^3}{16\sqrt{2}\,\alpha_1^2}-\frac{3\alpha_2\alpha_3}{2\sqrt{2}\,\alpha_1}+\frac{\sqrt{2}\alpha_2\alpha_5}{5\alpha_1^3}-\frac{9\alpha_4}{8\sqrt{2}}$$
$$+\frac{243\alpha_1^2\alpha_2}{320\sqrt{2}}+\frac{3\alpha_5}{5\alpha_1}+\frac{9\alpha_2^2}{16}-\frac{81\alpha_1^4}{640}\Big)\Big] \tag{A18}$$

$$P_4=\frac{4}{3\sqrt{2}}a_1^4(1-n)^3\Big[\Big(1-\frac{3\alpha_2^2}{4\alpha_1^4}-\frac{2\alpha_3}{\alpha_1^3}+\frac{3\alpha_4}{2\sqrt{2}\,\alpha_1^4}\Big)$$
$$+\gamma^2\Big(\frac{3\alpha_2^2}{\alpha_1^2}+\frac{4\alpha_3}{\alpha_1}+\frac{6\alpha_5}{5\alpha_1^3}-\frac{4\alpha_1^2}{5}-\frac{2\sqrt{2}\,\alpha_2\alpha_3}{\alpha_1^3}-\frac{3\sqrt{2}\,\alpha_4}{\alpha_1^2}\Big)$$
$$+\gamma^4\Big(\frac{\alpha_2^4}{4\alpha_1^4}+\frac{2\alpha_2^2\alpha_3}{\alpha_1^3}+\frac{\alpha_2\alpha_6}{2\alpha_1^4}-\frac{2\alpha_3^2}{3\alpha_1^2}-\frac{12\alpha_5}{5\alpha_1}-4\alpha_2^2$$
$$-\frac{8\alpha_1\alpha_3}{3}+\frac{4\alpha_1^4}{15}-\frac{\sqrt{2}\,\alpha_2\alpha_3^2}{3\alpha_1^4}-\frac{3\alpha_2^2\alpha_4}{2\sqrt{2}\,\alpha_1^4}-\frac{6\sqrt{2}\,\alpha_2\alpha_5}{5\alpha_1^3}$$
$$+\frac{\alpha_2^3}{\sqrt{2}\,\alpha_1^2}+\frac{4\sqrt{2}\,\alpha_2\alpha_3}{\alpha_1}+3\sqrt{2}\,\alpha_4+\frac{2\sqrt{2}\,\alpha_1^2\alpha_2}{15}\Big)\Big] \tag{A19}$$

$$Q_4=\frac{4}{3\sqrt{2}}a_1^4(1-n)^3\Big[\Big(1+\frac{3\alpha_2^2}{4\alpha_1^4}+\frac{2\alpha_3}{\alpha_1^3}-\frac{3\sqrt{2}\,\alpha_2}{\alpha_1^2}\Big)$$
$$+\gamma^2\Big(-\frac{3\alpha_2^2}{\alpha_1^2}-\frac{4\alpha_3}{\alpha_1}+\frac{6\alpha_5}{5\alpha_1^3}-\frac{4\alpha_1^2}{5}+4\sqrt{2}\,\alpha_2\Big)$$
$$+\gamma^4\Big(-\frac{\alpha_2^4}{4\alpha_1^4}-\frac{2\alpha_2^2\alpha_3}{\alpha_1^3}+\frac{\alpha_2\alpha_6}{2\alpha_1^4}-\frac{2\alpha_3^2}{3\alpha_1^2}-\frac{3\alpha_2\alpha_4}{\alpha_1^2}$$
$$-\frac{12\alpha_5}{5\alpha_1}+2\alpha_2^2+\frac{8\alpha_1\alpha_3}{3}+\frac{4\alpha_1^4}{15}+\frac{\sqrt{2}\,\alpha_6}{\alpha_1^2}$$
$$+\frac{3\alpha_2^3}{\sqrt{2}\,\alpha_1^2}+\frac{4\sqrt{2}\,\alpha_2\alpha_3}{3\alpha_1}-2\sqrt{2}\,\alpha_1^2\alpha_2\Big)\Big] \tag{A20}$$

This is the solution using the conventional or "old" treatment. The result of the new treatment is very simply obtained from it. The solution of the MI problem for the perfect region of the same shape as the sample is given by first putting $\gamma = 1$ and replacing a_1 by a_{10} in (A13)–(A20) and then phase smearing this result by introducing the factor γ^r into P_r and Q_r so that $(a_{10})^r$ returns to its original value a_1^r in (A13)–(A20). Thus the "new" treatment amounts simply to putting $\gamma = 1$ in (A13)–(A20) and we notice that the c_r and ψ_r of (6) are in that case independent of the Dingle temperature x.

The working of the scheme is illustrated by the examples below, which indicate the orders of magnitude involved and show that with the new treatment it is indeed necessary to go to high-order terms in order not to introduce appreciable errors in the c_r and ψ_r, especially at the lower temperature and for high r. The convergence is, however, much more rapid with the old treatment. Note, too, that the approximation used by Knecht is equivalent to retaining P_1, Q_1, P_2, and Q_2 and ignoring all terms multiplied by a power of γ^2 in (A13)–(A16); to this approximation the old and the new treatments are of course identical.

Examples of the Application of Equations (A13)–(A20)

The values of the α's are calculated assuming $F = 2.77 \times 10^8$ G and $m/m_0 = 1.24$.

1. $T = 1.203$ K, $H = 84.9$ kG, $G_1 = 0.42$, $n = 0.1$, $\alpha_1 = -0.520$, $\alpha_2 = 0.085$, $\alpha_3 = 0.012$, α_4, etc., negligible. We find

$$P_1 = a_1(1 - 0.019\gamma^2)$$

$$P_2 = [a_1^2(1-n)/\sqrt{2}](-0.554 - 0.046\gamma^2 + 0.009\gamma^4)$$

$$P_3 = (9/8)a_1^3(1-n)^2(-0.521 + 0.162\gamma^2 - 0.015\gamma^4)$$

$$P_4 = (4/3\sqrt{2})a_1^4(1-n)^3(1.096 - 0.189\gamma^2 + 0.001\gamma^4)$$

$$Q_1 = a_1(0.015\gamma^2 - 0.001\gamma^4)$$

$$Q_2 = [a_1^2(1-n)/\sqrt{2}](1 - 0.105\gamma^2 + 0.003\gamma^4)$$

$$Q_3 = (9/8)a_1^3(1-n^2)(-0.554 + 0.017\gamma^2 + 0.009\gamma^4)$$

$$Q_4 = (4/3\sqrt{2})a_1^4(1-n)^3(-0.431 + 0.277\gamma^2 - 0.045\gamma^4)$$

For the new treatment $\gamma^2 = 1$, for the old $\gamma^2 = 0.373$ if $x = 0.23$ K.

2. $T = 0.6$ K, $H = 84.0$ kG, $G_1 = 0.4$, $n = 0.08$, $\alpha_1 = -1.000$, $\alpha_2 = 0.609$, $\alpha_3 = 0.281$, $\alpha_4 = 0.007$. We find

$$P_1 = a_1(1 - 0.017\gamma - 0.037\gamma^4 + 0.002\gamma^6)$$

$$Q_1 = a_1(0.108\gamma^2 - 0.046\gamma^4 + 0.005\gamma^6)$$

For the old treatment, $\gamma^2 = 0.439$ if $x = 0.19$ K.

3. $T = 0.6$ K, $H = 40$ kG, $G_1 = 0.4$, $n = 0.08$, $\alpha_1 = 1.420$, $\alpha_2 = 0.221$, $\alpha_3 = 0.024$. We find

$$P_1 = a_1(1 - 0.213\gamma^2 + 0.011\gamma^4 - 0.001\gamma^6)$$

$$Q_1 = a_1(0.039\gamma^2 - 0.014\gamma^4 + 0.001\gamma^6)$$

For the old treatment $\gamma^2 = 0.177$ if $x = 0.19$ K.

ACKNOWLEDGMENTS

We should like to thank Mr. F. T. Sadler for help in the experiments; Dr. P. Kemp, Dr. J. P. Fitch, and Miss M. J. Day of the Cambridge University Computer Laboratory and Mr. W. M. Bibby for much valuable help with computing; and Prof. S. H. Vosko for valuable discussion and for supplying unpublished details of his calculations. One of us (J.M.P.) thanks the Science Research Council for a Senior Visiting Fellowship.

REFERENCES

1. D. L. Randles, *Proc. R. Soc. Lond. A* **331**, 85 (1972).
2. B. Knecht, *J. Low Temp. Phys.* **21**, 619 (1975).
3. D. Shoenberg and P. J. Stiles, *Proc. R. Soc. Lond. A* **281**, 62 (1964).
4. M. J. G. Lee, *Proc. R. Soc. Lond. A* **295**, 440 (1966).
5. B. Knecht, D. L. Randles, and D. Shoenberg, in *Low Temperature Physics—LT 13* (Plenum, New York, 1974), Vol. 4, p. 39.
6. D. L. Randles and M. Springford, *J. Phys. F* **3**, L185 (1973).
7. G. Dunifer, D. Pinkel, and S. Schultz, *Phys. Rev. B* **10**, 3159 (1974).
8. R. T. Schumacher and W. E. Vehse, *J. Phys. Chem. Solids* **24**, 297 (1963).
9. R. Dupree and E. F. W. Seymour, *Phys. Kondens. Materie* **12**, 97 (1970).
10. C. S. Barrett, *Acta Cryst.* **9**, 671 (1956).
11. R. W. Stark and L. R. Windmiller, *Cryogenics* **8**, 272 (1972).
12. R. A. Phillips and A. V. Gold, *Phys. Rev.* **178**, 932 (1969).
13. S. H. Vosko, J. P. Perdew, and A. H. MacDonald, *Phys. Rev. Lett.* **35**, 1725 (1975).
14. D. Shoenberg, *J. Low Temp. Phys.*, to be published.
15. W. M. Bibby, to be published.
16. D. Barton and J. P. Fitch, *Rep. Prog. Phys.* **35**, 235 (1972).
17. A. H. MacDonald and S. H. Vosko, private communication.